Volume 1 Issue 1

Trade Science Inc.

Research & Reviews On Polymer

Full Paper

RRPL, 1(1), 2010 [16-23]

Nonlinear viscoelasticity behavior testing of molten polymer in vibration force field

Juan Zhang*[1], Jin-Ping Qu[2]

[1]Department of Applied Mathematics, College of Science, Donghua University, Shanghai - 201620, (CHINA)

[2]National Engineering Research Center of Novel Equipment for Polymer Processing, South China University of Technology, Guangzhou - 510640, (CHINA)

E-mail : zhangjuan@dhu.edu.cn

Received: 19th March, 2009 ; Accepted: 24th March, 2009

ABSTRACT

The transient responses of polymer melts in vibration force field have been measured with the capillary dynamic rheometer, and the effects of the vibration parameters (vibration frequency and amplitude) on polymer melt's viscoelasticity have been presented and discussed.

KEYWORDS

Capillary dynamic rheometer;
Vibration force field;
Apparent viscosity;
Normal stress difference coefficient.

INTRODUCTION

Recently, the technique and the equipment of the electromagnetic dynamic plasticating extruder[1-3] for plastics have been recognized by academe and accepted extensively by industrial community. The electromagnetic dynamic plasticating extruder for plastics has acquired great economic and social benefit progressively. And there has been a great deal of research activity to investigate the behavior of polymers in vibration force field. In order to improve the design and control of various polymer-processing operations, this trend was promoted by the need to elucidate the complex dynamics of these viscoelastic fluids. Until now, from many experimental phenomena, it is the vibration force field that can affect the apparent viscosity and elasticity of polymer melts. But what is the effect? How to measure accurate data for the research? Experimentally, moreover, controlled transients are much more difficult to achieve than steady-state conditions.

One would like to have available the most versatile possible melt rheometer that can be measure the viscosity and elasticity properties of polymer melts. However, rheometer now in use is noted for their lack of versatility. The traditional capillary rheometer is used primarily to measure melt viscosity at high shear rates, while the first normal stress difference is determined by semi-empirical methods, from measurements of entrance pressure loss or exit pressure[4-6]. However, the validity of the method of analyzing the experimental data is subject to serious question, because some of the assumptions made for the suggested method do not have a proved justification. Although the rotational rheometer can be used to measure the elastic properties of polymer melts, it is limited by low shear rates due to flow instability. Therefore, for practical purposes, there is a need for a new capillary rheometer which can be used to measure nonlinear transient shear flow viscoelastic

properties not only in vibration force field but also in steady state. Fortunately, the capillary dynamic rheometer has been developed successfully in National Engineering Research Center of Novel Equipment for Polymer Processing in South China University of Technology, and this new rheometer has these capabilities[7-10]. In this paper, the effects of vibration parameters (including vibration frequency and amplitude) on the polymer melt's viscosity and normal stress difference coefficients are analyzed by obtainable transient data, which measured with the capillary dynamic rheometer.

THE CAPILLARY DYNAMIC RHEOMETER

This capillary dynamic rheometer is based on the capillary rheometer with invariable speed, and its equipment's physical model has good agreement with the pulsating extrusion process of round-section die in the condition of electromagnetic dynamic extrusion. One of the key technologies is that the mechanical vibration force field caused by an electromagnetic field is introduced into the whole plasticating and extrusion process. So the plasticating and extrusion for polymer melt is deeply affected by vibration force field. Figure 1 is the sketch map of capillary dynamic extrusion. The surrounding cylinder is isothermal clarifier. The material is calorified and then becomes the melt, which is extruded from the capillary with the high pressure by hydraulic driving. Here, a sine vibration can be added in parallel direction of polymer melt's flowing through capillary, so the periodic vibration force with high frequency and small amplitude is introduced into all the process of polymer melt extrusion through capillary. With the pressure transducer and the Laser-CCD real-time data acquisition system, the capillary entry pressure and the ratio of the swell can be measured instantaneously.

The equipment of the capillary dynamic rheometer includes electromagnetic vibration control system, capillary extruding system, barrel temperature control system, constant speed control system, entry pressure online collection system and the Laser-CCD real-time data acquisition system.

Figure 2 gives a block diagram of the vibration control system of piston rod. The frequency and amplitude signal set by a sine vibration control system is put on the power amplifier through the output knob, and these amplified signals are send to the equipment, then vibration is created. So vibration displacement or vibration velocity or vibration acceleration can be exported. At the same time, the mechanical energy is transformed to pressure signal by transducer, so the close control is realized.

It is a well-known fact that polymeric materials exhibit elastic properties when they are subjected to large deformations, especially in vibration force field their behavior is more complicated. There is ample evidence,

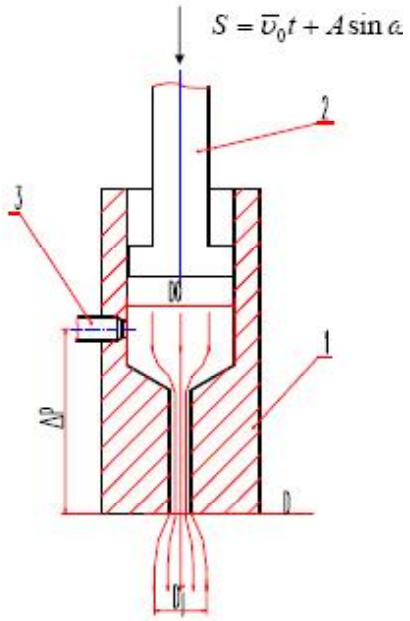

Figure 1 : Sketch map of capillary dynamic extrusion: 1: cylinder, 2: piston rod, 3: pressure transducer

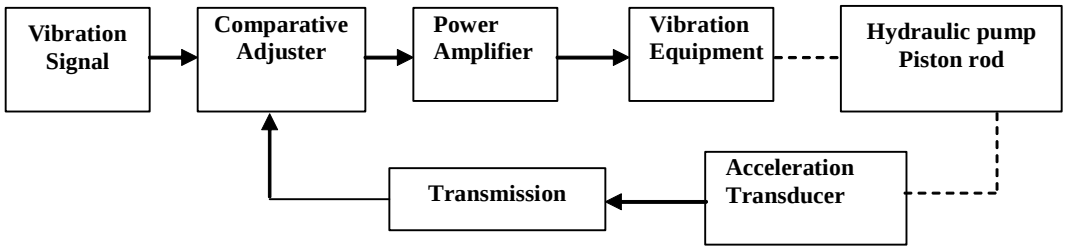

Figure 2 : Vibration control system of piston rod

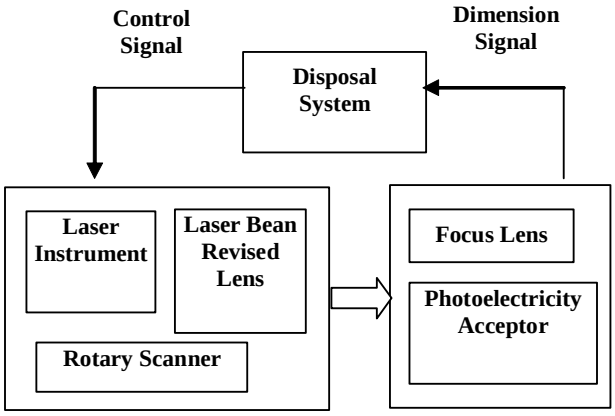

Figure 3 : Sketch map of laser measure instrument

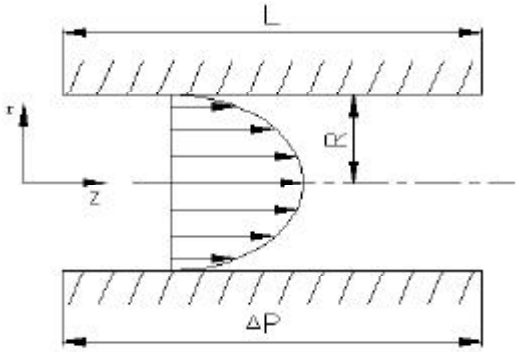

Figure 4 : Velocity of polymer melts in capillary dynamic rheometer (fully development section)

such as extrudate swelling, indicating that the melt elasticity plays a very important role in the various methods of processing polymeric materials. From recent developments in rheology it has been established that the melt elasticity is related to the normal stress differences, moreover there is a relationship between the normal stress differences and the extent of the die swell. For conveniently, we can measure the die-swell ratio with the Laser-CCD real-time data acquisition system. The Laser-CCD is laid in the exit of the die.

Figure 3 gives a block diagram of the laser measure instrument. Laser bean from laser instrument is revised by optics system and rips into the scanner that is circumvolving with the electromotor tail-wagging, therefore a parallel scanning light screen comes into being. When measured object is parked in the scanning screen, the projection is formed whose dimension is as same as the measured object. The scanning screen can be flocked to the photoelectricity acceptor after accepting focusing. Because the scanning screen is formed transiently, the wave on the photoelectricity acceptor can be reflected actually the complexion of parallel laser bean scanning with or without block. The impulse signal is transmitted into the disposal system through the circuit, the dimension of the measured object is obtained indirectly after disposing.

DATA ACQUISITION AND ANALYSIS

Figure 4 describes the velocity of polymer melts in capillary dynamic rheometer. Where L is the length of the capillary, R is the radius of the capillary, ΔP is the pressure difference between the two ports. The following assumptions will be made:

1. The melt flow is laminar in axial z-direction, and isothermal, and the ratio of L/2R is sufficiently great to ensure that a well-developed velocity profile;
2. The melt is uncompressible and viscoelastic, the density ρ is unchangeable;
3. Wall slip and gravitational effects may be neglected.

In capillary the velocity and the shear stress of the melt respectively are:

$$\mathbf{V} = \begin{bmatrix} V_z & 0 & 0 \end{bmatrix} \quad (1)$$

$$\tau = \begin{bmatrix} \tau_{zz} & \tau_{rz} & 0 \\ \tau_{rz} & \tau_{rr} & 0 \\ 0 & 0 & \tau_{\theta\theta} \end{bmatrix} \quad (2)$$

where boundary conditions are:

$$V_z(r,t)\big|_{r=R} = 0 \quad (3)$$

$$\tau_{rz}\big|_{r=0} = \text{const} \quad (4)$$

The displacement of the piston rod in capillary is:

$$S = \bar{\upsilon}_0 t + A\sin\omega t \quad (5)$$

where $\bar{\upsilon}_0$ is the steady average velocity of the piston rod, A is the vibration amplitude, ω is the vibration circle frequency (ω=2πf, f is vibration frequency).Through analyzing the movement equation and using conservation of mass, the average velocity in the capillary section can be described as:

$$\bar{\upsilon}_z = \left(\frac{R_0}{R}\right)^2 (\bar{\upsilon}_0 + A\omega\cos\omega t) \quad (6)$$

From the direction-z of the movement equation, it can be gained such as:

$$0 = \frac{\partial p}{\partial z} + \frac{1\partial}{r\partial r}(r\tau_{rz}) \quad (7)$$

Integrating above equation and predigesting it, then the shear stress of the capillary wall in Z-direction can be approximately described as:

$$\tau_R(t) \approx \frac{R\Delta P(t)}{2L} - \frac{\rho R_0^2 A\omega^2}{6R}.\sin\omega t = \frac{RP(t)}{2L} - \frac{2\rho\pi^2 R_0^2 Af^2}{3R}.\sin\omega t \quad (8)$$

In view of the shear rate of the capillary wall can be described as:

$$\dot{\gamma}_R = \frac{R_0^2}{R^3}(\bar{\upsilon} + A\omega\cos\omega t) \quad (9)$$

So the average apparent viscosity of the capillary wall can be described as:

$$\bar{\eta}_\alpha = \frac{\int_0^T \tau_R(t)dt}{T.\dot{\gamma}_R(t)} \quad (10)$$

With the on-line collection system, the capillary entry pressure can be measured instantaneously. Therefore the shear stress and the average apparent viscosity of the capillary wall in Z-direction can be obtained.

Figure 5 is the sketch map of extrudate swell, equation (6) describes the average velocity in section 1, in the same way, the average velocity $\overline{V}_j$ in section 2 can be described as:

$$\pi\rho R_j^2\overline{V}_j = \pi\rho R^2\overline{V_z} \quad (11)$$

supposed the die-swell ratio B is:

$$B = \frac{\pi R_j^2}{\pi R^2} = \frac{\overline{V}_j}{\overline{V}_z} \quad (12)$$

so there is:

$$\overline{V}_j = B^{-2}\overline{V}_z \quad (13)$$

The stress state of the melt in vibration shear force field may be written as follows:

$$\sigma_{ij} = -P\delta_{ij} + \tau_{ij} \quad (14)$$

When i=j, $\delta_{ij} = 1$; and when $i \neq j$, $\delta_{ij} = 0$. σ_{ij} is the component of the whole stress tensor, τ_{ij} is the component of the extra tensor, and $P = -\frac{1}{3}tr\sigma = -\frac{1}{3}(\sigma_{zz} + \sigma_{rr} + \sigma_{\theta\theta})$

The equation of motion in the radial direction can be rewritten as:

$$d(P - \tau_{rr}) = (\sigma_{rr} - \sigma_{\theta\theta})\cdot\frac{dr}{r} = N_2(r,t)d\ln r \quad (15)$$

where where $N_2(r,t) = \tau_{rr}-\tau\theta = \sigma_{rr}-\sigma\theta\theta$ is the second normal stress difference in the inner capillary where the radius is r. Integration of equation (15) from the centerline to any radius r yields:

$$P(r,z,t) - P(0,z,t) - \tau_{rr}(r,t) + \tau_{rr}(0,t) = \int_0^r N_2(r,t)d\ln r \quad (16)$$

When r=0, γ=0, that is to say, there is no annular elasticity stretchiness or no additive contractive force, so $\tau_{rr}(0,f) = 0$. From many experimental experience, the second normal stress difference is one quantitatively level smaller than the first normal stress difference, moreover, the second normal stress difference is negative. For conveniently, the suppose proposed by Weissenberg[11] can be used, which is: $N_2(r,f)=0$. Therefore equation (16) can be rewritten as:

$$P(r,z,t) = P(0,z,t) + \tau_{rr}(r,t) \quad (17)$$

The total pressure in the capillary thus consists of two parts: the hydrostatic pressure P(0,z,f) which decreases in the direction of flow, it can be supposed that P(0,z,f) = 0 because measuring is taken in the atmospheric pressure; and the 'elastic' pressure equals to $\tau_{rr}(0,f)$ which varies radially but is constant along the length of the capillary. So equation (17) becomes, at the downstream end of the capillary:

$$P(r,L,t) = \tau_{rr}(r,t) \quad (18)$$

Applying the continuity equation, the volume flux is:

$$Q = \pi R^2\overline{V}_z \quad (19)$$

Suppose:

$$V_z(r,t) = V_{max}[1 - (\frac{r}{R})^2] \quad (20)$$

There is

$$Q = 2\pi\int_0^R V_z r dr = 2\pi V_{max}\int_0^R [1-(r/R)^2]rdr = \frac{\pi}{2}R^2 V_{max} \quad (21)$$

From equation (19) and (21), there is:

$$V_{max} = 2\overline{V}_z \quad (22)$$

Applying Newton's second law to the portion of the fluid between Section 1 and Second 2 of Figure 5, the net external force, in the flow direction, will be equal to the rate of fluid momentum. The only external forces, in view of the assumptions made, will consist of the total stress in the flow direction, $\sigma_{zz}(r,L)$, acting at the Section 1, appropriately integrated over the entire cross section of the capillary, and one obtains:

$$\int_0^R 2\pi r\rho[V_z(r,t)]^2 dr - \pi R_j^2\rho V_j^2 = \int_0^R 2\pi r\sigma_{zz}(r,L,t)dr \quad (23)$$

and

$$\sigma_{zz}(r,L,t) = -P(r,L,t) + \tau_{zz}(r,t)$$
$$= \tau_{zz}(r,t) - \tau_{rr}(r,t) = N_1(r,t) \quad (24)$$

Therefore,

$$\int_0^R 2\pi r\rho[V_z(t)]^2 dr - B^{-2}\pi R^2 \overline{V}_z^2 = \int_0^R 2\pi r N_1(r,t) dr \quad (25)$$

Defined τ_R as the shear stress in the wall of the capillary, so,

$$\frac{r}{R} = \frac{\tau_{rz}}{\tau_R}, \; dr = \frac{R}{\tau_R} d\tau_{rz} \quad (26)$$

Substituting Eq. (26) into Eq. (25) and rearranging gives:

$$\frac{\rho \overline{V}_z^2}{2} \cdot B^{-2} + \frac{1}{\tau_R^2}\int_0^{\tau_R} \tau_{rz} \cdot \{N_1(\tau_{rz},t) - \rho[V_z(t)]^2\} \cdot d\tau_{rz} = 0 \quad (27)$$

If Eq. (27) is multiplied by τ^2_R and then differentiated with evaluating the individual terms of the Leibnitz rule. Carrying out this operation,

$$\frac{d}{d\tau_R}[\tau_R^2 \frac{\rho \overline{V}_z^2}{2} B^{-2}] + \tau_R \cdot N_1(R,t) - \frac{d}{d\tau_R}\{\int_0^{\tau_R} \tau_{rz} \cdot \rho[V_z(t)]^2 d\tau_{rz}\} = 0 \quad (28)$$

The third part of the left of Eq. (28) can be simplified:

$$\begin{aligned}
&\frac{d}{d\tau_R}\{\int_0^{\tau_R} \tau_{rz} \cdot \rho[V_z(t)]^2 d\tau_{rz}\} \\
&= \frac{d}{d\tau_R}\int_0^1 \rho V_z^2 \tau_R^2 (\frac{\tau_{rz}}{\tau_R}) d(\frac{\tau_{rz}}{\tau_R}) \\
&= \frac{d}{d\tau_R}\{\int_0^1 \rho V_z^2 \tau_R^2 (\frac{r}{R}) d(\frac{r}{R})\} \\
&= \frac{d}{d\tau_R}\{\int_0^1 \rho V_{max}^2 [1-(\frac{r}{R})^2]^2 \cdot \tau_R^2 (\frac{r}{R}) d(\frac{r}{R})\} \\
&= 2\tau_R \rho V_{max}^2 \{\int_0^1 [1-(\frac{r}{R})^2]^2 (\frac{r}{R}) d(\frac{r}{R})\} \\
&= \frac{\tau_R}{3}\rho V_{max}^2 = \frac{4}{3}\rho \tau_R \overline{V}_z^2
\end{aligned} \quad (29)$$

So Eq. (28) can be rewritten:

$$N_1(R,t) = \frac{4}{3}\rho \overline{V}_z^2 - \rho \overline{V}_z^2 B^{-2} = \rho \overline{V}_z^2 (\frac{4}{3} - B^{-2}) \quad (30)$$

and one can obtain the formula of the first normal stress difference in the wall of the capillary:

$$N_1(R,t) = \rho(\frac{4}{3} - B^{-2})(\frac{R_0}{R})^4 (\overline{\upsilon}_0 + A\omega\cos\omega t)^2 \quad (31)$$

So the average first normal stress difference coefficient can be obtained:

$$\psi 1 = \frac{\int_0^T N_1(f) dt}{T \cdot \dot{\gamma}_R^2(t)} \quad (32)$$

With the Laser-CCD real-time data acquisition system, the ratio of the swell can be measured instantaneously. With these data and equation (31), one can obtain the experimental values of the first normal stress difference and the average first normal stress difference coefficient in the wall of the capillary.

In our following experiment, the experimental material is LDPE and its melt temperature is 150 degrees centigrade.

Figure 6 is a plot of comparison of the experimental values of the shear stress with different vibration fre-

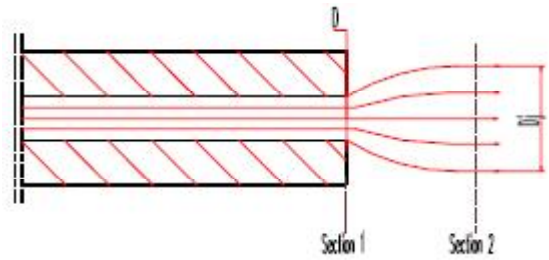

Figure 5: Sketch map of extrudate swell

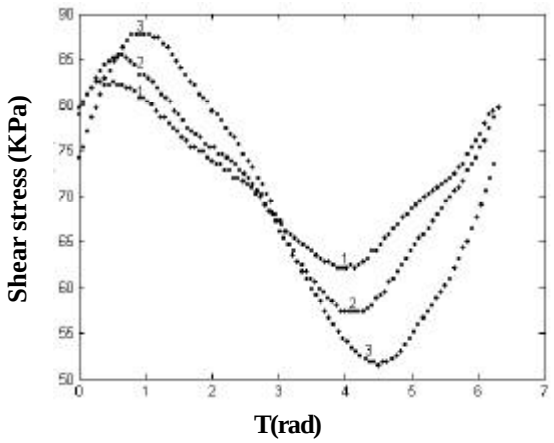

Figure 6 : Relationship between the experimental values of the shear stress and time with different vibration frequency in one period, A=0.1mm, T=ωt, $\overline{\upsilon}_0 = 15$ (mm/s), 1: f=6Hz, 2: f= 8 Hz, 3: f= 12Hz

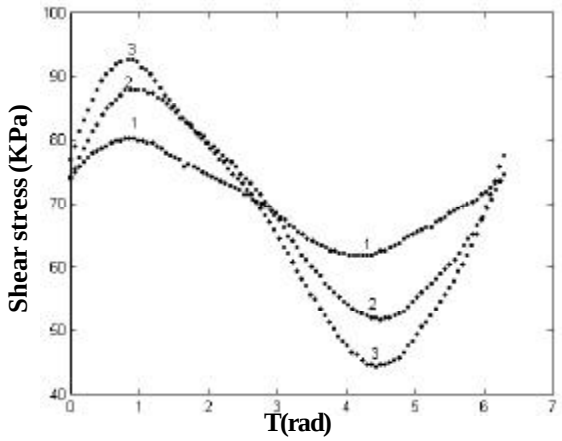

Figure 7 : Relationship between the experimental values of the shear stress and time with different amplitude in one period, f=10 Hz, $\bar{\upsilon}_0 = 15$ (mm/s), 1: A=0.05mm, 2: A=0.075 mm, 3: A=0.15mm

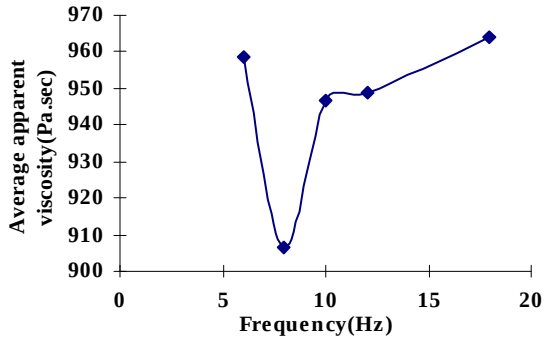

Figure 8: Experiment values of average apparent viscosity (Pa.sec) with A=0.1mm and $\bar{\upsilon}_0 = 15$ (mm/s)

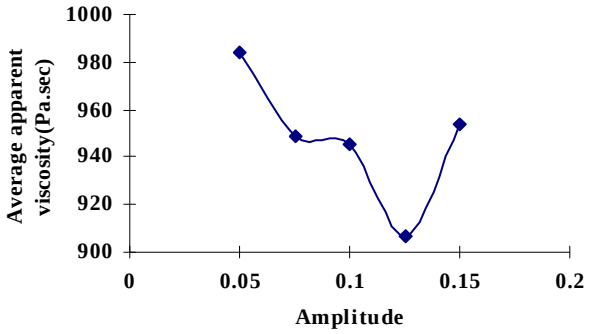

Figure 9 : Experiment values of average apparent viscosity (Pa.sec) with f=10 Hz and $\bar{\upsilon}_0 = 15$ (mm/s)

quency in one period. It is clear that the change amplitude of the shear stress increases with the vibration frequency increasing. Figure 7 is a plot of comparison of the experimental values of the shear stress with different amplitude in one period. It is also clear that the change amplitude of the shear stress increases with the vibration amplitude increasing. Maybe frequency or amplitude increasing means the intensity of the vibration force field being increased and the ability of overcoming viscoelastic resistance strengthened. Therefore the change amplitude of shear stress increases with frequency or amplitude increasing.

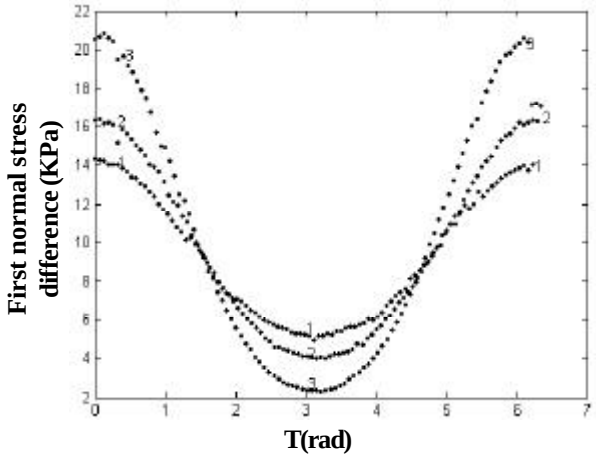

Figure 10 : Relationship between the experimental values of the first normal stress difference and time with different vibration frequency in one period, A=0.1mm, T=t, $\bar{\upsilon}_0 = 15$ (mm/s), 1: f=6 Hz, 2: f=8 Hz, 3: f=12 Hz

Figure 8 is a plot of the experiment values of the average apparent viscosity with constant amplitude and initial velocity. It is obvious that the relationship between the average apparent viscosity and the vibration frequency is nonlinear. When applied a low vibration frequency, the average apparent viscosity decreases rapidly, then there is an increase phenomenon with higher frequency. There is an optimum vibration frequency that minimized the average apparent viscosity of the polymer melt in the condition of the same amplitude.

Figure 9 is a plot of the experiment values of the average apparent viscosity with constant vibration frequency and initial velocity. It is also obvious that the relationship between the average apparent viscosity and the amplitude is nonlinear, and there is optimum amplitude, which also minimized the average apparent viscosity of the polymer melt in the condition of the same vibration frequency.

Figure 10 is a plot of the experimental values of first normal stress difference with different vibration frequency in one period. Figure 11 is a plot of the experimental values of first normal stress difference with different amplitude in one period. From these two figures, it is clear that the change amplitude of the first normal

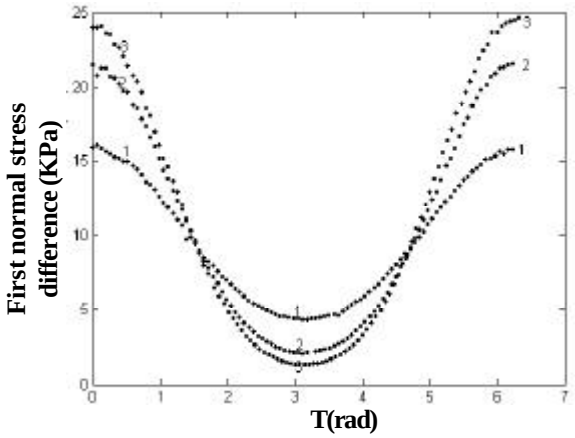

Figure 11: Relationship between the experimental values of the first normal stress difference and time with different amplitude in one period, T=ωt, f=6 Hz, $\bar{\upsilon}_0 = 15$ (mm/s), 1:A=0.075mm, 2: A= 0.125 mm, 3:A=0.15mm

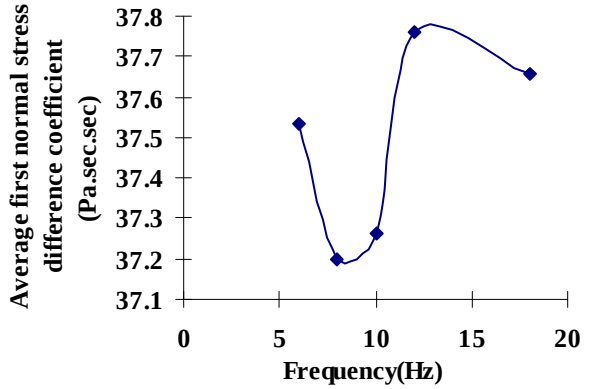

Figure 12: Experiment values of the average first normal stress difference coefficient (Pa.sec^2) with A=0.1mm and $\bar{\upsilon}_0 = 15$ (mm/s)

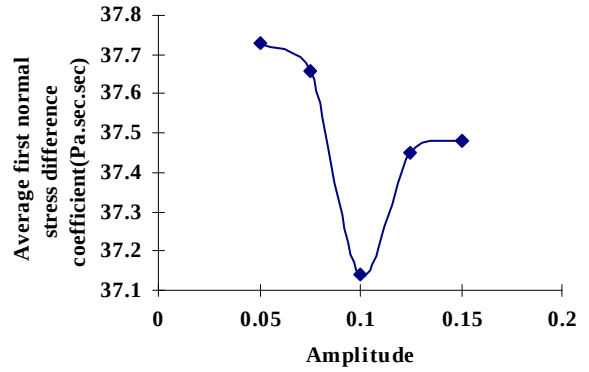

Figure 13: Experiment values of the average first normal stress difference coefficient (Pa.sec^2) with f= 10 Hz and $\bar{\upsilon}_0 = 15$ (mm/s)

stress difference increases with vibration frequency or amplitude increasing. Because the amplitude of shear rate increases with vibration frequency or amplitude increasing, then the decreasing amplitude of the entanglement density increases with frequency increasing, moreover, a decrease in the number of entangled points increases the average number of segments in polymeric chains, which causes as increase in free volume. The force between molecules decreases and the effect of the molecular orientation becomes stronger, which results in increasing of material's tensile strength and stiffness. So the change amplitude of the first normal stress difference increases, too. It is easy to conclude that the change amplitude of the elasticity of polymer melts increases with vibration frequency or amplitude increasing.

At the same time, figures 12 and 13 are the plots of the relationship between the experimental values of the average first normal stress difference coefficient and different vibration frequency and amplitude respectively. From figures 12 and 13, it is obviously conclude that the relationship between the average first normal stress difference coefficient and the vibration frequency or amplitude is nonlinear, and there is an optimum vibration frequency or amplitude, which also minimized the average first normal stress difference coefficient of the polymer melt in the condition of the same amplitude or vibration frequency.

CONCLUSION

In this work, using the capillary dynamic rheometer to measure the capillary entry pressure and the ratio of the swell instantaneously. The results can be presented the effects of the vibration parameters such as vibration frequency and amplitude. When vibration frequency or amplitude is larger, the change amplitude of the shear stress and the first normal stress difference both increases, therefore the change amplitude of the viscosity and elasticity of polymer melts increase with vibration frequency or amplitude increasing. At the same time, the relationship between the average apparent viscosity and the vibration frequency or amplitude is nonlinear, and the relationship between the average first normal stress difference coefficient and the vibration frequency or amplitude is also nonlinear, and there is an optimum vibration frequency or amplitude, which also minimized the average apparent viscosity or the average first normal stress difference coefficient of the polymer melt in the condition of the same amplitude or vibration frequency.

REFERENCES

[1] Jin-Ping Qu; Method and Equipment for Electromagnetic Dynamic Plasticating Extrusion of Polymer Materials, US Pat. 5217302, **(1993)**.

[2] Jin-Ping Qu; A Method and Equipment for the Electromagnetic Dynamic Plasticating Extrusion of Polymer, EP Pat. 0444306B1, **(1995)**

[3] Jin-Ping Qu; Plastics Electromagnetic Dynamic Plasticating Extrusion Machine (Award Lecture), 3rd International Conference on Manufacturing Technology, Hong Kong, **(1995)**.

[4] A.J.Giacomin, T.Samurkas, J.M.Dealy; Polym.Eng. Sci., **29**, 499-504 **(1989)**.

[5] T.Y.Liu, D.W.Mead, D.S.Soong, M.C.Williams; Rheologica Acta, **2**2, 81-89 **(1983)**.

[6] C.D.Han, M.Charles; Polym.Eng.Sci., **10(3)**, 148-153 **(1970)**.

[7] Juan Zhang; International Journal of Nonlinear Sciences and Numerical Simulation, **5(1)**, 37-44 **(2004)**.

[8] Juan Zhang; International Journal of Nonlinear Sciences and Numerical Simulation, **5(1)**, 97-98 **(2004)**.

[9] Juan Zhang, Jin-Ping Qu; Iranian Polymer Journal, **14(7)**, 609-615 **(2005)**.

[10] Juan Zhang, Jin-Ping Qu; Nonlinear Analysis, **63(5-7)**, e977-e984 **(2005)**.

[11] K.Weissenberg; Proceedings Second International Congress on Rheology. North-Holland, Amsterdam, 29 **(1949)**.